Rapid Inactivation of Depletion-activated Calcium Current (I_{CRAC}) Due to Local Calcium Feedback

ADAM ZWEIFACH and RICHARD S. LEWIS

From the Department of Molecular and Cellular Physiology, Stanford University School of Medicine, Stanford, California 94305

ABSTRACT Rapid inactivation of Ca^{2+} release-activated Ca^{2+} (CRAC) channels was studied in Jurkat leukemic T lymphocytes using whole-cell patch clamp recording and $[Ca^{2+}]_i$ measurement techniques. In the presence of 22 mM extracellular Ca^{2+}, the Ca^{2+} current declined with a biexponential time course (time constants of 8–30 ms and 50–150 ms) during hyperpolarizing pulses to potentials more negative than −40 mV. Several lines of evidence suggest that the fast inactivation process is Ca^{2+} but not voltage dependent. First, the speed and extent of inactivation are enhanced by conditions that increase the rate of Ca^{2+} entry through open channels. Second, inactivation is substantially reduced when Ba^{2+} is present as the charge carrier. Third, inactivation is slowed by intracellular dialysis with BAPTA (12 mM), a rapid Ca^{2+} buffer, but not by raising the cytoplasmic concentration of EGTA, a slower chelator, from 1.2 to 12 mM. Recovery from fast inactivation is complete within 200 ms after repolarization to −12 mV. Rapid inactivation is unaffected by changes in the number of open CRAC channels or global $[Ca^{2+}]_i$. These results demonstrate that rapid inactivation of I_{CRAC} results from the action of Ca^{2+} in close proximity to the intracellular mouths of individual channels, and that Ca^{2+} entry through one CRAC channel does not affect neighboring channels. A simple model for Ca^{2+} diffusion in the presence of a mobile buffer predicts multiple Ca^{2+} inactivation sites situated 3–4 nm from the intracellular mouth of the pore, consistent with a location on the CRAC channel itself.

INTRODUCTION

In many cells, the generation of inositol 1,4,5-trisphosphate (IP_3) by the engagement of cell surface receptors elicits both the release of Ca^{2+} from intracellular stores and the influx of Ca^{2+} across the plasma membrane (Berridge, 1993). In the case of T lymphocytes, this response is initiated by the binding of antigen to the T cell receptor, and results in a sustained rise in $[Ca^{2+}]_i$ that serves as an essential signal for T cell activation (Crabtree, 1989). Unlike intracellular Ca^{2+} release, which is controlled by a direct agonist action of IP_3 on its receptor in the endoplasmic

Address correspondence to Dr. Adam Zweifach, Beckman Center B-003, Stanford University School of Medicine, Stanford, CA 94305.

J. GEN. PHYSIOL. © The Rockefeller University Press · 0022-1295/95/02/0209/18 $2.00
Volume 105 February 1995 209–226

reticulum (ER) membrane, the activation of Ca^{2+} influx in most cases appears to result indirectly from the IP_3-dependent depletion of intracellular Ca^{2+} stores. This influx pathway, known as capacitative Ca^{2+} entry, is quite widespread (Putney, 1990). Strong evidence for capacitative Ca^{2+} entry in many cells, including T cells, comes from measurements with Ca^{2+}-sensitive dyes showing that depletion of Ca^{2+} stores by inhibitors of ER Ca^{2+}-ATPases can elicit Ca^{2+} influx without significant changes in [IP_3] (Gouy, Cefai, Christensen, Debre, and Bismuth, 1990; Putney, 1990; Mason, Garcia-Rodriguez, and Grinstein, 1991; Sarkadi, Tordai, Homolya, Scharff, and Gárdos, 1991; Putney and Bird, 1993).

More recently, electrophysiological studies with whole-cell recording techniques have revealed depletion-activated Ca^{2+} currents in a variety of cells (for reviews, see Fasolato, Innocenti, and Pozzan, 1994; Lewis and Cahalan, 1995). The most extensively characterized of these currents is known as I_{CRAC} (Ca^{2+} release-activated Ca^{2+} current) and has been described in mast cells (Hoth and Penner, 1992, 1993) and in T cells (Lewis and Cahalan, 1989; McDonald, Premack, and Gardner, 1993; Zweifach and Lewis, 1993; Premack, McDonald, and Gardner, 1994). Consistent with a role in mediating capacitative Ca^{2+} entry, I_{CRAC} is activated by several procedures that deplete intracellular Ca^{2+} stores, including intracellular dialysis with buffered solutions containing < 100 nM Ca^{2+}, intracellular application of IP_3, extracellular application of ionomycin, and treatment with thapsigargin or other ER Ca^{2+}-ATPase inhibitors. I_{CRAC} has been demonstrated to underlie T cell receptor-stimulated Ca^{2+} influx in T cells (Zweifach and Lewis, 1993; Premack et al., 1994). CRAC channels are highly selective for Ca^{2+} over monovalent cations, conduct Ca^{2+} better than Ba^{2+} or Sr^{2+}, and do not exhibit voltage-dependent gating (Lewis and Cahalan, 1989; Hoth and Penner, 1992, 1993; McDonald et al., 1993; Zweifach and Lewis, 1993; Premack et al., 1994). In addition, they have an extremely small unitary conductance, estimated from noise analysis to be ~ 10 fS under physiological conditions (Zweifach and Lewis, 1993). Together, these properties readily distinguish I_{CRAC} from other depletion-activated Ca^{2+} currents (Vaca and Kunze, 1993; Lückhoff and Clapham, 1994) and from receptor-operated, second-messenger–operated, or voltage-gated Ca^{2+} currents (Tsien and Tsien, 1990).

Ca^{2+}-dependent inactivation is a well documented mechanism that provides feedback control over the amplitude and kinetic behavior of some types of voltage-gated Ca^{2+} channels (Eckert and Chad, 1984). Interestingly, evidence from several studies indicates that intracellular Ca^{2+} also feeds back to inhibit I_{CRAC} on two very different time scales. A slow inactivation process, occurring over tens of seconds, is suggested by the observations that elevation of extracellular [Ca^{2+}] only transiently increases the magnitude of I_{CRAC} (Lewis and Cahalan, 1989; Zweifach and Lewis, 1993), and that photolytic release of intracellular caged calcium diminishes the current (McDonald et al., 1993). This slow inactivation process results in part from refilling of intracellular Ca^{2+} stores (Zweifach and Lewis, 1994). A second, more rapid inactivation process inhibits I_{CRAC} on a millisecond time scale during hyperpolarizing voltage pulses (Hoth and Penner, 1992, 1993). This fast inactivation was suggested to be Ca^{2+} dependent, as replacement of EGTA in the recording pipette with the faster chelator BAPTA (1,2-bis(2-aminophenoxy) ethane *N,N,N'N'*-tetraacetic acid) reduced its extent. Rapid negative feedback by intracellular Ca^{2+} may provide an

important safeguard that limits the amplitude of Ca^{2+} signals particularly during membrane hyperpolarization, while slow feedback is likely to participate in the generation of dynamic behavior. In T cells, slow negative feedback by Ca^{2+} is thought to play a major role in generating fluctuations of capacitative Ca^{2+} entry that underlie antigen-receptor-stimulated $[Ca^{2+}]_i$ oscillations (Lewis and Cahalan, 1989; Donnadieu, Bismuth, and Trautmann, 1992; Dolmetsch and Lewis, 1994).

In this paper, we describe the characteristics of rapid I_{CRAC} inactivation with the aim of elucidating its mechanism. The results show that fast inactivation is driven by the flux of Ca^{2+} through individual channels, and that the channel density and current amplitude are small enough that inactivation of each channel proceeds independently of its neighbors. Furthermore, the different effects of intracellular EGTA and BAPTA on fast inactivation support a model by which Ca^{2+} binds to nearby inactivation sites probably located on the CRAC channel itself. Portions of this work have been published in abstract form (Zweifach and Lewis, 1994).

METHODS

Cells and Materials

Jurkat E6-1 human leukemic T cells were maintained in complete medium containing RPMI 1640 and 10% heat-inactivated fetal bovine serum, 2 mM glutamine, and 25 mM HEPES, in a 6% CO_2 humidified atmosphere at 37°C. Log-phase cells ($0.2–1.2 \times 10^6$/ml) were allowed to settle onto but not firmly adhere to glass coverslips shortly before each experiment. Thapsigargin (LC Pharmaceuticals, Woburn, MA) was prepared as a 1 mM stock solution in DMSO. Cs_4BAPTA was purchased from Molecular Probes, Inc. (Eugene, OR).

Whole-Cell Recording

Patch clamp experiments were conducted in the standard whole-cell recording configuration (Hamill, Marty, Neher, Sakmann, and Sigworth, 1981). Extracellular Ringer's solution contained (in millimolar): 155 NaCl, 4.5 KCl, 1 $MgCl_2$, 10 D-glucose, and 5 Na-HEPES (pH 7.4), with $CaCl_2$ or $BaCl_2$ added to give the desired final concentration. 3 mM $MgCl_2$ was used in Ca^{2+}-free Ringer's. Internal solutions contained (in millimolar): 140 Cs aspartate, 10 Cs-HEPES (pH 7.2) and either 0.66 $CaCl_2$/11.68 EGTA/3.01 $MgCl_2$ (high EGTA solution), 0.066 $CaCl_2$/1.2 EGTA/2.01 $MgCl_2$ (low EGTA solution), or 0.90 $CaCl_2$/12.0 BAPTA/3.16 $MgCl_2$ (BAPTA solution). The free $[Ca^{2+}]$ of all internal solutions, measured with indo-1, was 5 nM; the calculated free $[Mg^{2+}]$ was 2 mM. Recording electrodes were pulled from 100-μl pipettes (VWR, West Chester, PA), coated with Sylgard® near their tips, and fire polished to a resistance of 2–8 MΩ when filled with Cs aspartate pipette solution. The patch clamp output (Axopatch 200, Axon Instruments, Inc., Foster City, CA) was filtered at 1.5 kHz with an 8-pole Bessel filter (Frequency Devices, Inc., Haverhill, MA) and digitized at a rate of 5 kHz. Stimulation and recording were performed with an Apple Macintosh computer driving an ITC-16 interface (Instrutech Corp., Elmont, NY) and using PulseControl software extensions (Jack Herrington and Richard Bookman, University of Miami, FL) to Igor Pro (WaveMetrics, Inc., Lake Oswego, OR). Command potentials were corrected for the −12 mV junction potential that exists between the aspartate-based pipette solutions and Ringer's solution. We did not compensate for the series resistance, which ranged from 5–25 MΩ and for the current amplitudes in this study (< 100 pA) would be expected to cause voltage errors of < 3 mV. External solutions were changed by positioning the cell ~1 mm inside one barrel of a perfusion-tube array through which the desired solution flowed (< 0.1 ml/min). Experiments were conducted at 22–25°C.

Immediately after gigaseal formation, each cell was exposed to Ca^{2+}-free Ringer's solution and suction was applied to establish the whole-cell configuration. Leak currents were then obtained under Ca^{2+}-free conditions by applying hyperpolarizing steps of the same amplitude and duration as subsequent test hyperpolarizations (see below). In experiments where a family of voltage steps of varying amplitude were applied, single leak traces were collected at each potential. In experiments where steps to a single potential were given, five leak traces were collected and averaged. After 3 min, $[Ca^{2+}]_o$ was elevated to 2–22 mM and 200-ms hyperpolarizing pulses were delivered from a holding potential of −12 mV every 2 s (unless noted otherwise) in order to measure I_{CRAC}. This I_{CRAC} activation protocol, consisting of incubation in Ca^{2+}-free Ringer's and intracellular dialysis with $[Ca^{2+}]_i < 10$ nM for 3 min, was sufficient for maximal activation; additional pretreatment with 1 μM thapsigargin did not further increase the average initial size of I_{CRAC}. With the exception of Fig. 1, all sweeps were corrected for the leak conductance (20–100 pS) recorded in the absence of Ca_o^{2+}. Peak currents were measured from a 1-ms average beginning 3 ms after the start of the pulse to minimize contributions from uncompensated capacitative current (time constant <1 ms). Steady state currents were measured as a 5–10-ms average at the end of the pulse. The time course of current decay was fitted by a biexponential function using Igor Pro.

Indo-1 $[Ca^{2+}]_i$ Measurements

For experiments combining patch clamp recording with $[Ca^{2+}]_i$ measurements, cells were preloaded with 1 μM indo-1/AM (Molecular Probes, Inc.) in complete medium for 30 min at 37°C, washed twice with medium, and stored in the dark at 22–25°C until use. In addition, pipette solutions were supplemented with 100 μM indo-1 pentapotassium salt (Molecular Probes, Inc.). Cells were illuminated using a 75-W xenon arc lamp, a 360 ± 5 nm interference filter (Omega Optical, Brattleboro, VT) and a 380-nm dichroic mirror (Chroma Technology Corp., Brattleboro, VT) mounted on a Nikon Diaphot inverted microscope equipped with a Nikon Fluor 40× objective (NA 1.3). A TTL-controlled shutter (Uniblitz, Rochester, NY) was used to control the duration of illumination. The emission signal was collected from an area slightly larger than the cell that included a small portion of the pipette. Emitted light was split with a 440-nm dichroic mirror and passed through 405 ± 15 nm and 485 ± 12.5 nm interference filters (Chroma Technology Corp.) to two photomultiplier tubes (HCl24-02, Hamamatsu Corp., Bridgewater, NJ). The PMT outputs were low-pass filtered at 1.5 kHz and averaged over 90 ms for each data point. The fluorescence intensity due to the indo-1 in the pipette was measured by subtracting the fluorescence of the loaded cell alone from the fluorescence intensity of the cell plus the pipette after establishing the cell-attached configuration. Pipette fluorescence and the average autofluorescence of unloaded cells was subtracted from subsequent fluorescence values before calculation of the 405/485 ratio R. $[Ca^{2+}]_i$ was estimated from the relation $[Ca^{2+}]_i = K^* (R\text{-}R_{min})/(R_{max}\text{-}R)$, where K^*, R_{min}, and R_{max} are values determined from in vivo calibrations similar to those described previously for fura-2 (Lewis and Cahalan, 1989). Briefly, R_{min} and R_{max} were measured ~5 min after establishing the whole-cell configuration with Cs aspartate pipette solutions containing 100 μM indo-1 and either 10 mM EGTA (for R_{min}) or 10 mM $CaCl_2$ (for R_{max}). For R_{min} measurements, cells were bathed in Ca^{2+}-free Ringer's to avoid increases in $[Ca^{2+}]_i$ resulting from activation of I_{CRAC}. K^* was determined from the R values of cells loaded with a solution containing 100 μM indo-1, 10 mM total EGTA, and 137 nM free Ca^{2+} as determined from in vitro indo-1 measurements (assuming a K_d of 250 nM for indo-1). The in vivo calibration values were (mean ± SD, $n = 3$): $R_{min} = 0.36 \pm 0.02$, $R_{max} = 4.67 \pm 0.35$, and $K^* = 1.2 \times 10^{-6} \pm 0.12 \times 10^{-6}$. These values differed significantly from those measured using the same solutions in vitro ($R_{min} = 0.084$, $R_{max} = 1.79$, and $K^* = 1.09 \times 10^{-6}$, presumably due to effects of the cytosolic microenvironment on the properties of indo-1.

RESULTS

Two Kinetically Distinct Components of I_{CRAC} *Inactivation*

Previous work has shown that I_{CRAC} can be induced by intracellular dialysis with low-Ca^{2+} solutions, presumably due to depletion of cellular Ca^{2+} stores (Lewis and Cahalan, 1989; Hoth and Penner, 1992; Zweifach and Lewis, 1993; Premack et al., 1994). In the study described here, we maximally activated CRAC channels by

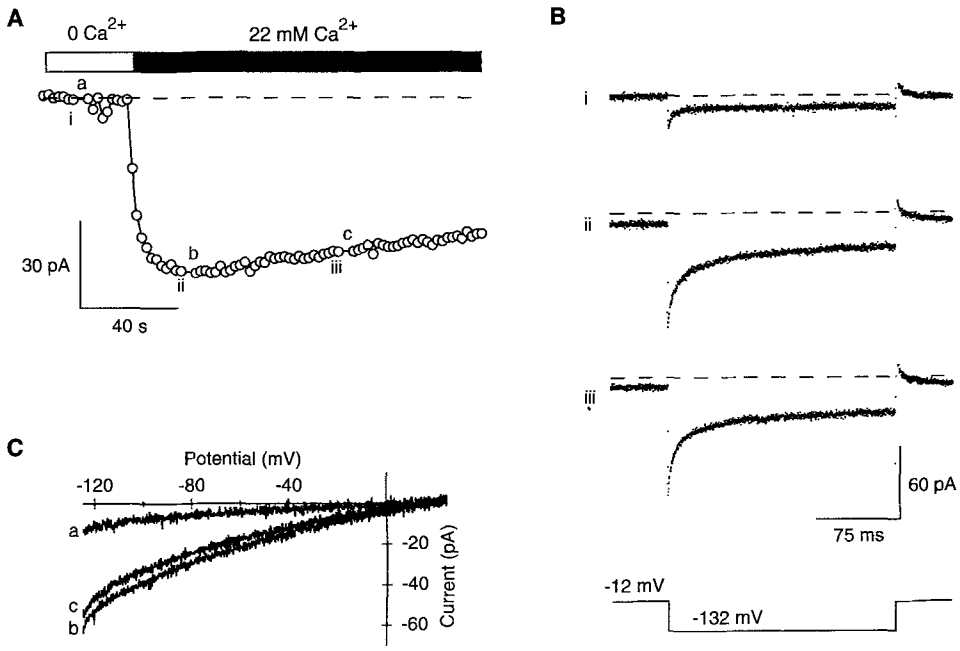

FIGURE 1. Fast inactivation of I_{CRAC}. (*A*) After depletion of intracellular Ca^{2+} stores in Ca^{2+}-free Ringer's (*open bar*), exposure to 22 mM Ca_o^{2+} (*solid bar*) reveals an inward Ca^{2+} current (I_{CRAC}) that is largely sustained over the course of ~120 s. The plot shows peak currents measured during hyperpolarizing voltage steps applied every 2 s as shown in *B* (see Methods). Times indicated by *i–iii* and *a–c* mark the collection times for data shown in *B* and *C*, respectively. (*B*) Responses to 200-ms voltage pulses from −12 to −132 mV collected at the times indicated by *i–iii* in *A*. During each pulse, the current is initially large but decays substantially due to fast inactivation. (*Dashed lines*) 0-current level. These data were not leak corrected. (*C*) Currents elicited by voltage ramps from −125 to +25 mV are shown at times *a–c* during the experiment shown in *A*. The current-voltage relations show that the currents seen in *A* and *B* are due solely to I_{CRAC}. Internal solution: Cs aspartate + 12 mM EGTA.

internal dialysis of Jurkat T cells for 3 min with EGTA- or BAPTA-buffered low-Ca^{2+} solutions ($[Ca^{2+}]_{free}$ = 5 nM) in the presence of extracellular Ca^{2+}-free Ringer's (see Methods). Peak inward current was monitored during hyperpolarizing pulses from −12 to −132 mV delivered every 2 s; the peak current amplitudes derived from individual pulses (Fig. 1 *B*) are plotted on a slow time scale in Fig. 1 *A*. In the absence of Ca_o^{2+}, hyperpolarization evoked only leak current (trace *i*). Subsequent exposure to

22 mM Ca_o^{2+} produced an inward Ca^{2+} current that was identified as I_{CRAC} on the basis of its inwardly rectifying current-voltage relation (Fig. 1 *C*), Ca^{2+} selectivity, lack of voltage-dependent gating, sensitivity to Ni^{2+} block, and lack of visible noise. As indicated in Fig. 1 *C*, contamination by voltage- or Ca^{2+}-dependent K^+ currents (Grissmer, Lewis, and Cahalan, 1992) or volume-activated Cl^- currents (Lewis, Ross, and Cahalan, 1993) was effectively prevented in these experiments by including Cs^+ but not ATP in the pipette and ensuring that the internal solution was hypotonic with respect to external solutions.

The inward current decays rapidly during hyperpolarizing voltage steps due to a process that we refer to as rapid inactivation (Fig. 1 *B*). In cells dialyzed with a moderate amount of EGTA (1.2 mM), $[Ca^{2+}]_i$ gradually rises and causes a ~1000-fold slower decay of the current (Zweifach and Lewis, 1994). This slow inhibition of I_{CRAC} occurs independently of fast inactivation (see Fig. 7 below) and will be described in detail elsewhere (Zweifach and Lewis, manuscript in preparation).

Kinetics of Fast Inactivation

The time course of fast inactivation was investigated under conditions of heavy intracellular Ca^{2+} buffering (12 mM $EGTA_i$), which maintained I_{CRAC} at a constant size throughout the duration of the experiment. I_{CRAC} decayed with a biexponential time course during hyperpolarizing pulses more negative than −40 mV in the presence of 22 mM Ca_o^{2+} (Fig. 2, *A* and *B*). Overall, the speed of inactivation increased with hyperpolarization between −82 and −162 mV as shown in Fig. 2 *B*; this was due to an acceleration of the fast exponential component (from τ = 30 to 8 ms) and the slower component (from τ = 150 to 50 ms), as well as to an increase in the relative contribution of the faster component to the current's decay. The overall effect of fast inactivation is to reduce the voltage dependence of I_{CRAC} at negative potentials. While peak current rises monotonically with increasing hyperpolarization, the amplitude of the steady state current increases only slightly between −50 and −100 mV and actually declines with further hyperpolarization (Fig. 2 *C*). The extent of inactivation at each potential was calculated from the peak (I_p) and steady state (I_{ss}) current values as $1 - I_{ss}/I_p$. In the potential range studied, the extent of inactivation was a nearly linear function of voltage (Fig. 2 *B*) and peak current (Fig. 2 *D*). Interestingly, the relation of inactivation to the steady state current is non-monotonic; inactivation increases with hyperpolarization below −100 mV, even as the steady state current decreases (Fig. 2 *D*).

Recovery from fast inactivation occurred at a rate similar to its development. The time course of recovery was measured using a two-pulse protocol in which steps from −12 to −132 mV were delivered with a variable interpulse interval at −12 mV. As shown in Fig. 3 *A*, the peak current amplitude during the second pulse increased with time of recovery. The time course in six cells was biexponential with average time constants of 9 ms (30% of total amplitude) and 75 ms (70% of total amplitude) (Fig. 3 *B*). The time course of recovery was not affected by substitution of BAPTA for EGTA in the pipette (data not shown). However, recovery was accelerated somewhat at a more positive potential (+50 mV), and was largely suppressed at a more negative one (−50 mV, not shown).

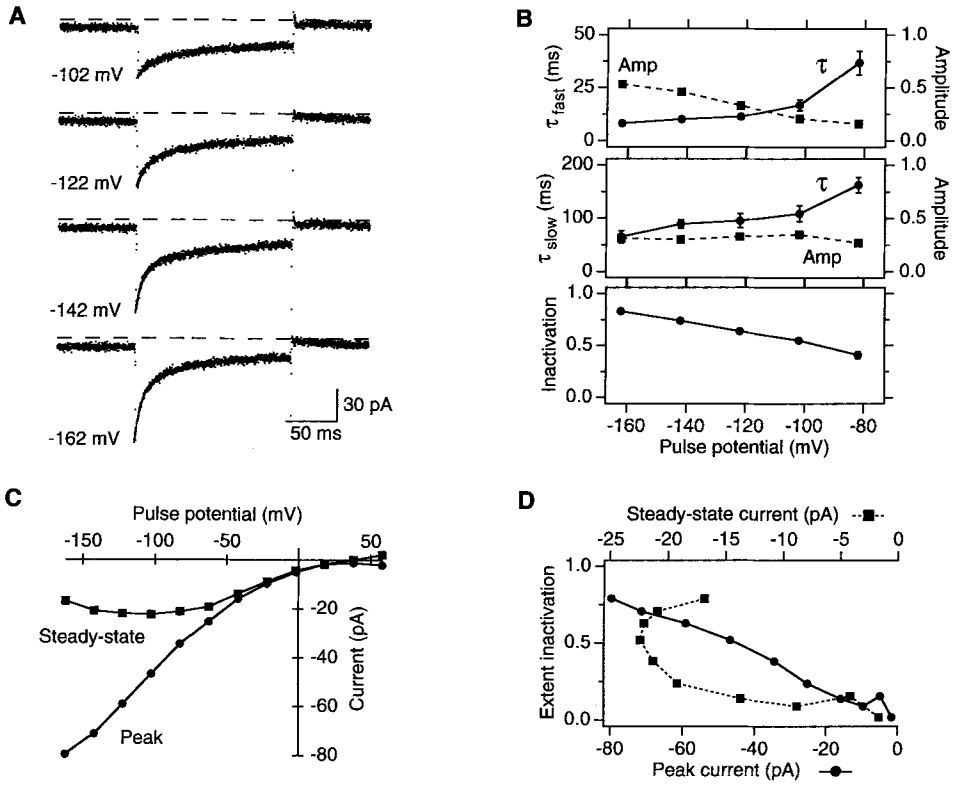

FIGURE 2. Kinetics of fast inactivation. (*A*) Responses of one cell to a graded series of hyperpolarizing pulses to the voltages indicated from a holding potential of −12 mV. Superimposed on the data are biexponential fits described by the function $I = I_0 + A_1e^{-t/\tau 1} + A_2e^{-t/\tau 2}$. (*B*) Average inactivation fitting parameters plotted against pulse potential. The apparent voltage dependence of A and τ for the fast (*top graph*) and slow (*middle graph*) components are shown; both components contribute to the overall extent of inactivation during each pulse ($1 - I_{ss}/I_p$) plotted in the bottom graph. Mean values ± SEM are shown ($n = 7$ cells). Where error bars are not visible, they are smaller than the symbol. (*C*) Current-voltage relation for the peak and steady state currents for the cell shown in *A*. (*D*) Extent of inactivation plotted as a function of the peak and steady state current. Inactivation values were calculated as $1 - I_{ss}/I_p$ from the data in *C*. Inactivation is a monotonic function of peak but not steady state current. Internal solution: Cs aspartate + 12 mM EGTA.

Fast Inactivation Is Calcium but Not Voltage Dependent

The apparent voltage dependence of fast inactivation seen in Fig. 2 could in principle arise from strictly voltage-dependent or Ca^{2+}-dependent processes, both of which have been described for voltage-gated Ca^{2+} channels in excitable cells (Eckert and Chad, 1984). We investigated the contribution of these two mechanisms in several ways: by varying the rate of Ca^{2+} influx independently of membrane potential, by changing the current carrier from Ca^{2+} to Ba^{2+}, and by varying the intracellular buffering of Ca^{2+} and therefore, the local $[Ca^{2+}]_i$ near the channels.

At all potentials tested, the extent of inactivation increased as $[Ca^{2+}]_o$ was raised from 2 mM to 6 or 22 mM (Fig. 4, *A* and *B*), primarily due to an increase in the contribution of the faster component to the inactivation process. These effects are unlikely to be due to changes in surface potential, as identical results were obtained in experiments in which Mg^{2+} was used to hold constant the total divalent ion concentration. The results are consistent with an effect of Ca^{2+} itself on fast inactivation, but do not address its physical site of action nor do they rule out additional contributions from membrane potential.

The role of Ca^{2+} influx through single channels was assessed by replotting the inactivation data of Fig. 4 *B* as a function of the estimated single-channel current amplitude. The unitary conductance of CRAC channels is too small for single-channel currents to be detected, but the unitary current size at −80 mV has been

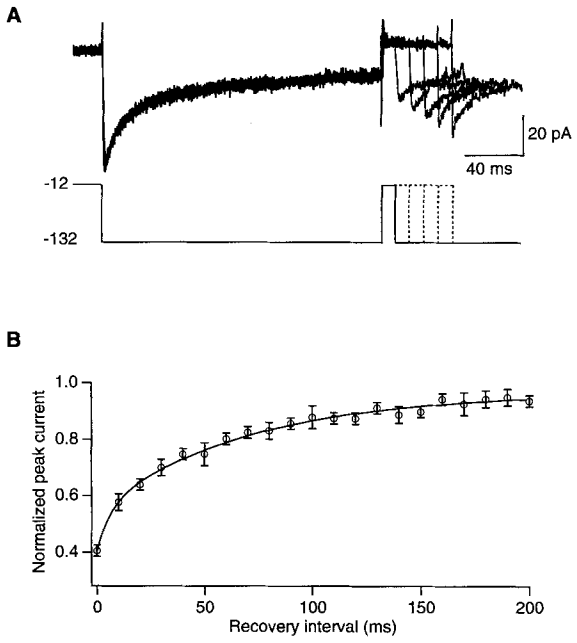

FIGURE 3. Recovery from fast inactivation. (*A*) After a 200-ms conditioning pulse to −132 mV to induce inactivation, the cell was depolarized to −12 mV for variable periods followed by a second pulse to −132 mV. Five consecutive responses collected every 10 s are superimposed. (*B*) Peak current during the second pulse (I_{p2}), normalized to the peak current during the first pulse (I_{p1}), is plotted against the recovery interval. Data points are the mean ± SEM for six cells. The recovery time course was fitted by the function $I_{p2}/I_{p1} = 1 - A_1e^{-t/\tau 1} - A_2e^{-t/\tau 2}$, where τ_1 = 9 ms, A_1 = 0.3, τ_2 = 75 ms, and A_2 = 0.7. Internal solution: Cs apartate + 12 mM EGTA.

estimated from noise analysis to be −1.5 fA with 2 mM Ca_o^{2+} (Zweifach and Lewis, 1993) or −3.5 fA with 22 mM Ca_o^{2+} (A. Zweifach, unpublished observations). The peak current (I_p) attained at each voltage is the product of the number of open channels, which was held constant throughout the experiment by high intracellular Ca^{2+} buffering, and the single-channel current (i_{Ca}). Therefore, i_{Ca} was calculated for each potential by scaling the unitary current estimate for 2 or 22 mM Ca_o^{2+} by the ratio of I_p at that potential to I_p at −80 mV measured in the same cell. As shown in Fig. 4 *C*, a plot of the extent of inactivation against estimated i_{Ca} describes a single, saturating relationship, supporting the notion that inactivation is driven by the Ca^{2+} flux through single channels. Moreover, because the data obtained in the presence of 2 mM Ca_o^{2+} and 22 mM Ca_o^{2+} follow the same relationship, we conclude that I_{CRAC} inactivation exhibits little or no direct voltage dependence.

Inactivation of currents carried by Ba^{2+} through CRAC channels was studied to examine further the Ca^{2+} and voltage sensitivity of this process. As illustrated in Fig. 5, Ba_o^{2+} substitution for Ca_o^{2+} reduced both the current amplitude and the extent of inactivation measured during hyperpolarizing pulses. The diminished inactivation of I_{CRAC} with Ba^{2+} as the permeant ion further supports the conclusion that fast inactivation is not directly voltage dependent.

The site of inactivation by Ca^{2+} was studied by measuring the effects of intracellular Ca^{2+} buffers having different Ca^{2+} binding rates (Fig. 6). Elevation of $EGTA_i$ from

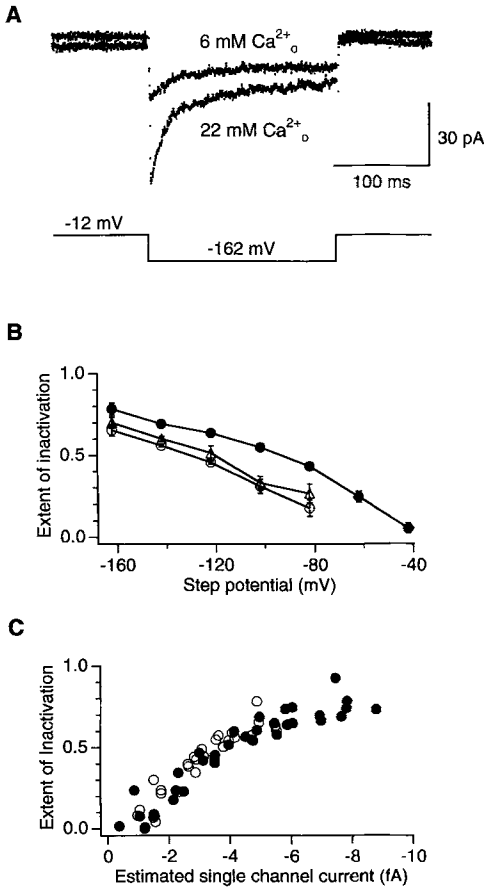

FIGURE 4. Dependence of inactivation on extracellular $[Ca^{2+}]$. (*A*) Current responses to hyperpolarizing voltage steps obtained with 6 and 22 mM Ca_o^{2+} from the same cell. Internal solution: Cs apartate + 12 mM EGTA. (*B*) The extent of fast inactivation plotted against potential for 200-ms hyperpolarizing steps. Data show mean values ± SEM for 4–6 cells in the presence of 22 mM (●), 6 mM (△), or 2 mM (○) Ca_o^{2+}. At all potentials, increasing $[Ca^{2+}]_o$ enhances inactivation. Internal solutions: Cs apartate + 12 mM EGTA. (*C*) The extent of inactivation is a function of the single-channel current amplitude. Single-channel current amplitudes were estimated from noise analysis and peak current amplitudes as described in the text, using the data summarized in *B* (○, 2 mM Ca_o^{2+}; ●, 22 mM Ca_o^{2+}). The data describe a single saturating relationship between single-channel current amplitude and the extent of inactivation regardless of $[Ca^{2+}]_o$, indicating that the inactivation mechanism is not voltage dependent.

1.2 to 12 mM had no discernable effect on fast inactivation at any potential (Fig. 6 *B*). However, 12 mM $BAPTA_i$, a chelator with ~400-fold faster Ca^{2+}-binding kinetics (Tsien, 1980; Adler, Augustine, Duffy, and Charlton, 1991), significantly slowed inactivation and reduced its extent at all potentials. $BAPTA_i$ also altered the kinetics of inactivation such that the current decayed with a single-exponential time course at all but the most hyperpolarized potentials (−162 mV). These data provide strong evidence that cytosolic Ca^{2+} plays a role in fast inactivation, and suggest that the essential Ca^{2+} binding site resides a short distance from the mouth of the channel.

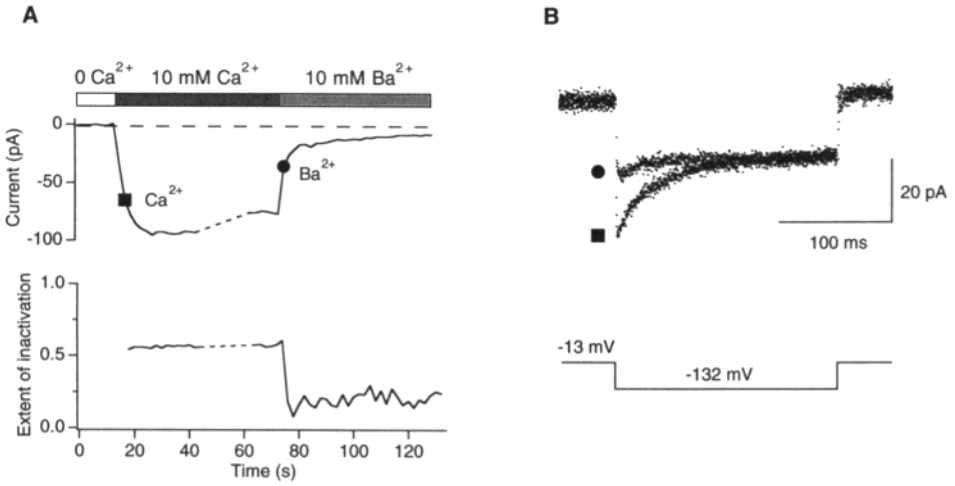

FIGURE 5. Ba^{2+} current inactivates less than Ca^{2+} current. (*A*) Comparison of inactivation in the presence of 10 mM Ca_o^{2+} and 10 mM Ba_o^{2+}. Peak current amplitude (*top graph*) and the extent of inactivation during hyperpolarizing steps from −12 to −132 mV (*bottom graph*) were measured every 2 s. 180 s after break in, the cell was exposed to 10 mM Ca^{2+}-Ringer's. During the period indicated by the dashed lines, a series of steps to more hyperpolarized potentials was applied, causing a small reduction in current amplitude when pulses to −132 mV were resumed. Exposure to 10 mM Ba^{2+} immediately reduced the current amplitude and the extent of inactivation. Symbols show the times at which the traces in *B* were collected. (*B*) Selected current responses to hyperpolarizing voltage steps obtained in 10 mM Ca_o^{2+} (■) or 10 mM Ba_o^{2+} (●). Pipette solution: Cs aspartate + 12 mM EGTA.

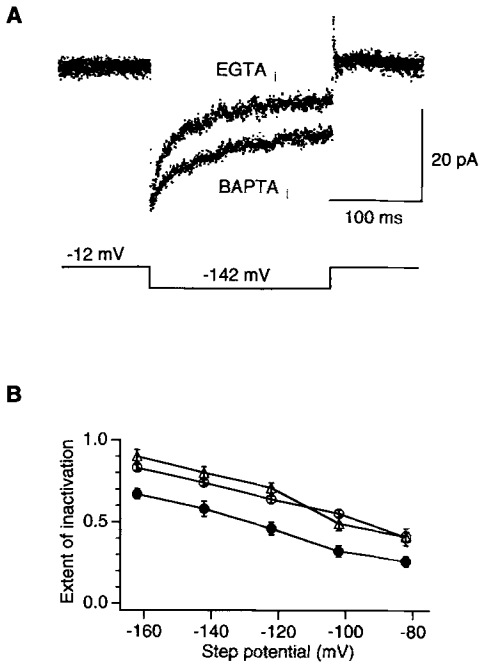

FIGURE 6. Effects of exogenous intracellular Ca^{2+} buffers on fast inactivation. (*A*) Current responses to hyperpolarizing steps obtained in 22 mM Ca_o^{2+} with 12 mM $BAPTA_i$ or 12 mM $EGTA_i$. Data were selected from two cells displaying approximately equal peak current amplitudes. (*B*) Extent of inactivation plotted against step potential for several intracellular buffering conditions. Increasing $[EGTA]_i$ from 1.2 mM (△) to 12 mM (○) does not affect the extent of fast inactivation at any potential, but 12 mM BAPTA (●) diminishes it. Data are mean ± SEM from four to six cells.

CRAC Channels Inactivate Independently of Each Other

In excitable cells, the unitary conductance and surface density of Ca^{2+} channels is in some cases sufficiently high that Ca^{2+} entering through one channel can enhance the Ca^{2+}-dependent inactivation of neighboring channels (Imredy and Yue, 1992). Because increasing the number of open channels reduces the average distance between sites of Ca^{2+} influx, overlapping Ca^{2+} domains are indicated by an enhanced inactivation occurring in parallel with increasing activation. We tested whether Ca^{2+} domains near CRAC channels overlap by examining fast inactivation under condi-

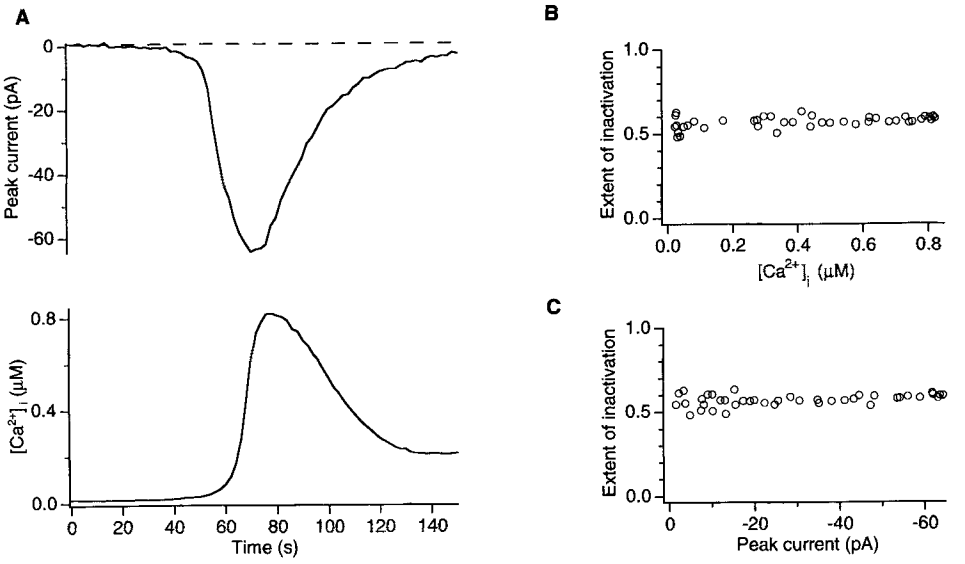

FIGURE 7. Fast inactivation is governed by local Ca^{2+} feedback within nonoverlapping single-channel domains. (*A*) Whole-cell dialysis with low [EGTA] (1.2 mM) slowly activates I_{CRAC} (*top trace*) in the presence of 22 mM Ca_o^{2+}, causing a rise in $[Ca^{2+}]_i$ (*lower trace*) and a slow decline in I_{CRAC} as channels close. Peak current during hyperpolarizing pulses to −132 mV are plotted every 2 s as in Fig. 1 *A*. (*B*) The extent of fast inactivation monitored during 200-ms steps from −12 to −132 mV is unaffected by increases in global $[Ca^{2+}]_i$ up to 0.8 μM. (*C*) The extent of inactivation is independent of changes in peak whole-cell Ca^{2+} current. Thus, inactivation is not dependent on the number of open channels, implying that neighboring single-channel Ca^{2+} domains do not overlap. All data are from the same experiment. Internal solution: Cs aspartate + 1.2 mM EGTA + 100 μM indo-1.

tions where the number of open channels was allowed to change while the driving force for Ca^{2+} entry was held constant. I_{CRAC} was activated in the presence of 22 mM Ca_o^{2+} by intracellular dialysis with 1.2 mM EGTA (free $[Ca^{2+}]_i$ = 5 nM). As the current slowly developed, hyperpolarizing voltage steps to −132 mV were applied every 2 s to monitor the rate and extent of fast inactivation, and $[Ca^{2+}]_i$ was measured using indo-1. As shown in Fig. 7 *A*, $[Ca^{2+}]_i$ rose in parallel with the development of inward Ca^{2+} current, then fell as I_{CRAC} declined due to a Ca^{2+}-dependent slow inhibition process (Zweifach and Lewis, 1994). However, during this entire period the extent of

fast inactivation evoked by hyperpolarizing voltage pulses was constant. Thus, fast inactivation depends on neither the global $[Ca^{2+}]_i$ (Fig. 7 *B*) nor the number of open CRAC channels (Fig. 7 *C*). Similar results were obtained when I_{CRAC} amplitude was reduced by SKF 96365, a compound that inhibits capacitative Ca^{2+} entry in a variety of cell types (Mason, Mayer, and Hymel, 1992). Over a period of 60 s, 100 μM SKF 96365 inhibited I_{CRAC} by ~80% without affecting the rate or extent of fast inactivation. Together with the results of the preceding section, these results indicate that fast inactivation is governed only by the electrochemical driving force for Ca^{2+} entry, and that Ca^{2+} entry through one channel does not affect its neighbor. Thus, we conclude that fast inactivation results from the action of incoming Ca^{2+} in private microdomains near the mouth of each CRAC channel.

DISCUSSION

Fast Inactivation Is Controlled by Local Calcium Feedback

Our data support the idea that fast inactivation of I_{CRAC} is a Ca^{2+}-dependent rather than a voltage-dependent process. A purely voltage-dependent process would be inconsistent with the observed sensitivity of inactivation to $[Ca^{2+}]_o$ (Fig. 4), the nature of the permeant ion (Fig. 5), and the species of intracellular buffer (Fig. 6). The relation of inactivation to the estimated single-channel current is independent of $[Ca^{2+}]_o$ and voltage (Fig. 4 *C*), indicating that the apparent Ca_o^{2+} and voltage dependence of fast inactivation can be explained through effects on the driving force for Ca^{2+} entry. Although the residual inactivation observed with Ba_o^{2+} (Fig. 5) might be attributed to slight voltage dependence, it could also be explained by some ability of Ba^{2+} to substitute for Ca^{2+} in causing inactivation. For example, Ba^{2+} has been shown to be effective (although less effective than Ca^{2+}) in opening Ca^{2+}-activated Cl^- currents in *Xenopus* oocytes (Neely, Olcese, Wei, Birnbaumer, and Stefani, 1994).

Several lines of evidence indicate that fast inactivation results from local rather than global increases in $[Ca^{2+}]_i$, implying that the relevant binding site is close to the channel. First, the extent of inactivation is unaffected by large changes in the number of open CRAC channels or global $[Ca^{2+}]_i$ (Fig. 7), indicating a lack of overlap between single-channel Ca^{2+} domains. The notion of microdomains of Ca^{2+} accumulation was originally developed to describe the Ca^{2+}-dependent inactivation of voltage-gated Ca^{2+} channels in *Aplysia* neurons (Chad and Eckert, 1984), and microdomain models have been applied to predict $[Ca^{2+}]_i$ profiles near Ca^{2+} channels at synapses (Simon and Llinas, 1985; Smith and Augustine, 1988; Roberts, 1993) and in pancreatic β-cells (Sherman, Keizer, and Rinzel, 1990). As for CRAC channels, inactivation of voltage-gated Ca^{2+} channels in several preparations appears to depend on the single-channel amplitude but not on the number of open channels (Chad and Eckert, 1984; Sherman et al., 1990; Neely et al., 1994). In T cells, the fact that Ca^{2+} entering one channel does not affect inactivation of its neighbors may be explained by the relatively low single-channel current (~10- to 100-fold smaller than voltage-gated Ca^{2+} channels), the proximity of the binding site to the channel (see below), and the average spacing of the channels (~100 nm, assuming a uniform distribution of ~10^4 channels/cell; Zweifach and Lewis, 1993). A second argument in favor of local feedback is the nonmonotonic relation between inactivation and I_{ss} in

experiments in which the number of open channels is constant (Fig. 2 *D*). If fast inactivation were controlled by global $[Ca^{2+}]_i$, an equilibrium should exist at every potential between I_{ss} and the extent of inactivation, leading to a monotonic relation between the two. Instead, inactivation increases monotonically with I_p, which is consistent with the dependence of inactivation on single-channel Ca^{2+} flux (Fig. 4 *C*). Finally, fast inactivation is sensitive to the species of intracellular Ca^{2+} buffer. Fast inactivation is not affected by reducing $EGTA_i$ from 12 to 1.2 mM, but is diminished by 12 mM $BAPTA_i$ (Fig. 6), consistent with the fact that BAPTA is a faster buffer than EGTA, as discussed below. The ability of $BAPTA_i$ to affect inactivation indicates that the Ca^{2+} binding site is exposed to the cytoplasm rather than residing within the pore.

Predicting the Location of the Ca^{2+} Binding Site(s) for Fast Inactivation

The different efficiencies with which intracellular EGTA and BAPTA reduce inactivation can be used to estimate the location of the Ca^{2+} binding site(s). A rough estimate can be made by considering the mean distance Ca^{2+} diffuses from the entry site before binding to the buffer. The mean path length of free Ca^{2+}, λ, can be expressed as (Neher, 1986; Roberts, 1993):

$$\lambda = (D_{Ca}/(k_{on}B))^{1/2} \quad (1)$$

where D_{Ca} is the Ca^{2+} diffusion coefficient ($\sim 3 \times 10^{-10}$ m^2 s^{-1}), k_{on} is the forward rate constant of the buffer ($k_{on} = 6 \times 10^8$ M^{-1} s^{-1} for BAPTA; $k_{on} = 1.5 \times 10^6$ M^{-1} s^{-1} for EGTA at pH 7.2; Tsien, 1980; Adler et al., 1991), and B is the buffer concentration. λ is 129 nm in the presence of 12 mM $EGTA_i$ and 6.5 nm in the presence of 12 mM $BAPTA_i$. Because inactivation is diminished by $BAPTA_i$ but not by $EGTA_i$, this places the inactivation binding site(s) closer to 6 nm than to 129 nm from the channel pore.

Theoretical models of Ca^{2+} diffusion in the presence of exogenous intracellular Ca^{2+} buffers predict that a steady state $[Ca^{2+}]_i$ gradient will form rapidly near the mouth of each channel, within μs of channel opening (Chad and Eckert, 1984; Simon and Llinas, 1985; Neher, 1986). For the case of a highly mobile, nonsaturable intracellular buffer, the following relation approximates the steady state distribution of Ca^{2+} as a function of r, the distance from the mouth of the pore (Neher, 1986):

$$[Ca^{2+}](r) = [Ca^{2+}]_\infty + \frac{i_{Ca}}{4\pi F r D_{Ca}} \exp(-r/\lambda) \quad (2)$$

where $[Ca^{2+}]_\infty$ is the bulk cytosolic $[Ca^{2+}]$ (5 nM), F is Faraday's constant, and D_{Ca}, i_{Ca}, and λ are as defined above. This model makes several critical assumptions. First, it assumes an infinite supply of a highly mobile exogenous chelator, such that the buffer does not saturate even close to the pore. This condition is satisfied by the fact that i_{Ca} is small (≤ 10 fA), and that the buffers are highly mobile (D for BAPTA and EGTA are close to D_{Ca}) and concentrated (1.2–12 mM). Within a 5-nm radius of the channel, the mean $[Ca^{2+}]_i$ is estimated to be ~ 8 μM (see below), and the average concentration of free buffer exceeds this by >100- to 1000-fold. Therefore, local saturation of the buffer is unlikely. Second, this model ignores the effects of endogenous buffers, both fixed and mobile. The absence of fixed buffer terms is

justified by the fact that nondiffusible buffers cannot influence $[Ca^{2+}]_i$ in the steady state. The effects of diffusible endogenous buffers in T cells is likely to be small, because the Ca^{2+} binding capacity (κ) of endogenous buffers in T cells has been estimated to be 125 (Donnadieu et al., 1992), or >500-fold lower than the binding capacity of 12 mM BAPTA (Neher, 1988). Third, the effect of Ca^{2+} extrusion by plasma-membrane ATPases is ignored, because they are unlikely to export significant amounts of Ca^{2+} over the molecular distance scale under consideration here. Finally, the model is based on the condition that $[Ca^{2+}]_i$ at each distance from the channel is at steady state, i.e., $\partial[Ca^{2+}]/\partial t = 0$. The steady state condition does not apply in the close vicinity of a single channel over short time periods. The average time it takes a Ca^{2+} ion to escape from a 5-nm radius domain by diffusion (0.014 μs) is much smaller than the mean time between ion entry events (32 μs, based on a maximal i_{Ca} of −10 fA); thus, the average number of Ca^{2+} ions within this domain is only 0.014/32, or 4×10^{-4}. However, even though the number of Ca^{2+} ions in the domain is always $\ll 1$, the fact that each channel inactivates independently (Fig. 7) makes it valid to consider the summed or averaged concentration of a large ensemble of channel domains simultaneously. The whole-cell currents being measured here are probably generated by >10,000 CRAC channels (Zweifach and Lewis, 1993), a sufficiently large number that the ensemble average $[Ca^{2+}]_i$ in small domains can attain the steady state condition required by the model.

The model predicts that $[Ca^{2+}]_i$ gradients will form in extremely localized microdomains surrounding CRAC channels. Fig. 8 *A* illustrates the predicted profile of $[Ca^{2+}]$ for distances ≤20 nm from the channel mouth under several different conditions. The dashed curve shows the predicted gradient in the absence of exogenous chelator for $i_{Ca} = -3.3$ fA, a simulation of Ca^{2+} influx at −122 mV in the presence of 2 mM Ca_o^{2+}. The inclusion of 12 mM $EGTA_i$ under these conditions has little effect on $[Ca^{2+}]_i$ near the channel, as is expected given the relatively slow capture rate for EGTA and the correspondingly large space constant λ of 129 nm. Substitution of $BAPTA_i$ for $EGTA_i$ steepens the gradient by shortening the Ca^{2+} capture time and the associated space constant ($\lambda = 6$ nm). The binding site(s) for Ca^{2+} can be roughly localized by inspecting the $[Ca^{2+}]_i$ profiles in Fig. 8 *A* predicted for 12 mM $EGTA_i$ ($i_{Ca} = -3.3$ fA) and 12 mM $BAPTA_i$ ($i_{Ca} = -5.5$ fA), conditions that elicit ~45% inactivation. The binding site(s) must lie near the intersection of the two curves; i.e., ~4 nm from the mouth of the channel.

Because $BAPTA_i$ substitution for $EGTA_i$ changes the shape of the $[Ca^{2+}]$ profile near open channels (Fig. 8 *A*), the predicted Ca^{2+} dependence of inactivation with the two different buffers can be used to determine a unique location for the Ca^{2+} binding site(s). The model was used to calculate $[Ca^{2+}]_i$ at a distance of 10 or 3 nm from the channel mouth, using estimated values for i_{Ca} at voltages of −162 to −82 mV in the presence of 22 mM or 2 mM Ca^{2+} (see Fig. 4 *C*). These values of $[Ca^{2+}]_i$ were then plotted against the corresponding measured mean values of the extent of inactivation. If the site (or sites) are assumed to lie 10 nm from the mouth of the pore (Fig. 8 *B*, *left*), the model predicts that inactivation is more sensitive to Ca_i^{2+} in the presence of $BAPTA_i$ than with $EGTA_i$. However, if the binding sites are assumed to be only 3 nm from the mouth of the pore (Fig. 8 *B*, *right*), then the same Ca^{2+} dependence is predicted for the two buffering conditions. Because it is unlikely that the species of Ca^{2+} buffer alters the intrinsic Ca^{2+} sensitivity of inactivation, we

conclude that the Ca^{2+} binding site or sites are likely to be 3–4 nm from the mouth of the pore. Assuming CRAC channel dimensions similar to those of other Ca^{2+} channels (Smith and Augustine, 1988), this location implies that the binding site or sites are part of the channel itself. In addition, the Ca^{2+} sensitivity of inactivation is best described by the Hill equation with a coefficient of 2.04 (Fig. 8 *B*), implying that multiple Ca^{2+} ions bind in order to cause inactivation. The existence of multiple Ca^{2+} binding sites is consistent with the biexponential time course of inactivation (Fig. 2 *A*)

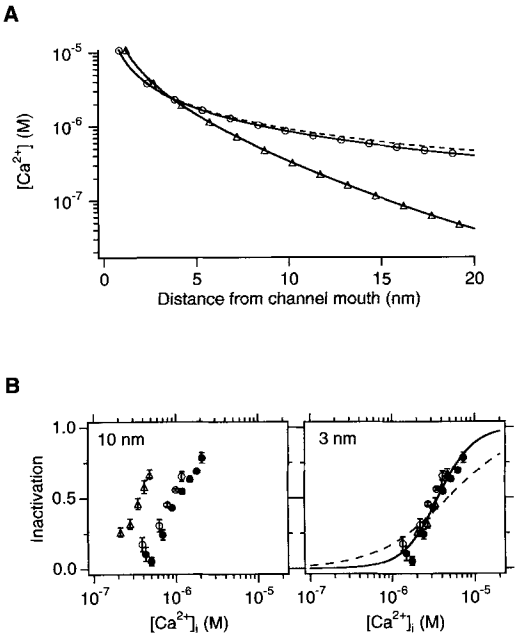

FIGURE 8. Estimating the location and properties of the Ca^{2+} binding site(s) for fast inactivation. (*A*) $[Ca^{2+}]_i$ calculated as a function of distance from a point source of Ca^{2+} influx (see text). $[Ca^{2+}]_i$ profiles are illustrated for three conditions: $i_{Ca} = -3.3$ fA without exogenous Ca^{2+} buffer (--) or with 12 mM $EGTA_i$ (○), and $i_{Ca} = -5.5$ fA with 12 mM $BAPTA_i$ (△). The EGTA and BAPTA conditions produce the same level of inactivation (~45%) measured experimentally. (*B*) The extent of inactivation plotted against the estimated local $[Ca^{2+}]_i$ at distances of 10 and 3 nm from the channel mouth. Inactivation values were taken from Figs. 4 *B* and 6 *B*. For each of these points, single-channel current amplitude was estimated from peak I_{CRAC} amplitude as in Fig. 4 *C*, and these values were used to estimate $[Ca^{2+}]_i$ at 10 nm and 3 nm from the channel mouth (see text). Experimental conditions were 12 mM $BAPTA_i$, 22 mM Ca_o^{2+} (△); 12 mM $EGTA_i$, 22 mM Ca_o^{2+} (●); 12 mM $EGTA_i$, 2 mM Ca_o^{2+} (○). An equation of the form $1 - I_{ss}/I_p = ([Ca^{2+}]^n/(K_d^n + [Ca^{2+}]^n)$ has been fitted to the EGTA data for $r = 3$ nm by a nonlinear least-squares criterion (*right graph*). The fitting parameters were: $n = 1$, $K_d = 4.8 \times 10^{-6}$ M (*dashed line*); $n = 2.04$, $K_d = 3.6 \times 10^{-6}$ M (*solid line*). The model predicts the same Ca^{2+} sensitivity of inactivation in the presence of either $EGTA_i$ or $BAPTA_i$ only if the binding site is assumed to be located 3–4 nm from the mouth of the channel.

and recovery from inactivation (Fig. 3 *B*), although other underlying causes are also possible.

Several uncertainties may affect the accuracy of the model's predictions. First, the model assumes Ca^{2+} diffusion from a point source into an infinite volume, which may not accurately describe the conditions that exist in extremely close proximity to a channel protein. For example, diffusion barriers, perhaps arising from the channel architecture itself, may create a restricted space near the mouth of the pore. Restricted diffusion would increase $[Ca^{2+}]_i$ near the channel and could conceivably violate assumptions about nonsaturation of the buffers. Restricted diffusion caused by close apposition of sarcoplasmic reticulum and plasma membranes has been sug-

gested to affect activation of Ca^{2+} release channels in smooth muscle (Kargacin, 1994). However, no analogous supporting evidence exists as yet for CRAC channels in T cells. Second, inaccurate estimates of i_{Ca} will induce corresponding errors in $[Ca^{2+}]$. Noise analysis commonly underestimates the true single-channel conductance (Fenwick, Marty, and Neher, 1982), and although I_{CRAC} fluctuations appeared to be well resolved in a previous study (Zweifach and Lewis, 1993), a severalfold underestimate cannot be ruled out. An error of this sort would affect only the inferred Ca^{2+} sensitivity of inactivation but not the estimated location of the Ca^{2+} binding site nor the degree of cooperativity. Interestingly, in some experiments, global $[Ca^{2+}]_i$ attained levels as high as 5 μM without increasing the extent of inactivation, even though the model predicts that it should (Fig. 8 *C*). This discrepancy could be explained by a severalfold underestimate of the true single-channel current amplitude or by restricted diffusion near the pore. Lastly, an error in the value for D_{Ca} will affect the estimated location of the Ca^{2+} binding sites. A reasonable upper limit for D_{Ca} is the Ca^{2+} diffusion coefficient in water, or 6×10^{-10} m^2/s (Robinson and Stokes, 1965). This assumption for D_{Ca} would shift the binding site to ~8 nm from the channel mouth. Recent measurements in Ca^{2+}-saturated *Xenopus* oocyte cytoplasm indicate a somewhat lower D_{Ca} of 2.2×10^{-10} m^2 s^{-1} (Allbritton, Meyer, and Stryer, 1992) presumably due to the tortuosity of cytoplasm; this value is close to our assumed value.

Possible Functions of Rapid I_{CRAC} Inactivation

Fast inactivation is likely to exert a significant effect on I_{CRAC} under physiological conditions by reducing the voltage sensitivity of Ca^{2+} influx at potentials at or below the resting level (−50 to −70 mV). For example, hyperpolarization from −50 to −80 mV in the presence of 2 mM Ca_o^{2+} would be expected to double the single-channel current amplitude based on peak current measurements like those in Fig. 2 *C*. However, ~20% of the current is inactivated at −80 mV (Fig. 4 *B*), thus reducing the increase in whole-cell I_{CRAC} from 100 to 60%. Hyperpolarizations of this size have been observed due to the opening of Ca^{2+}-activated K^+ channels in T cells with elevated $[Ca^{2+}]_i$ (Grinstein and Smith, 1989). At physiological Ca_o^{2+} levels, fast inactivation is insignificant at potentials above −60 mV; hence, it is not likely to influence the apparent voltage dependence of Ca^{2+} entry in cells depolarized from rest. In view of its rapid kinetics, fast inactivation is unlikely to play a significant role in generating slow periodic changes in I_{CRAC} amplitude that underlie $[Ca^{2+}]_i$ oscillations in T cells (Dolmetsch and Lewis, 1994). Nevertheless, by reducing the voltage dependence of Ca^{2+} influx during hyperpolarization, fast inactivation may diminish the role of Ca^{2+}-activated K^+ channels in the oscillation mechanism. The fact that a similar fast inactivation process was observed in mast cells (Hoth and Penner, 1993) suggests it is a general feature of CRAC channels.

We would like to thank Ricardo Dolmetsch, Chris Fanger, and Drs. Rick Aldrich and Markus Hoth for helpful discussions. Supriya Kelkar provided valuable assistance with cell culture.

This work was supported by NRSA postdoctoral fellowship AI08568 (to A. Zweifach) and NIH Grant GM47354 (to R. S. Lewis).

Original version received 14 July 1994 and accepted version received 19 October 1994.

REFERENCES

Adler, E. M., G. J. Augustine, S. N. Duffy, and M. P. Charlton. 1991. Alien intracellular calcium chelators attenuate neurotransmitter release at the squid giant synapse. *Journal of Neuroscience.* 11:1496–1507.

Allbritton, N. L., T. Meyer, and L. Stryer. 1992. Range of messenger action of calcium ion and inositol 1,4,5-trisphosphate. *Science.* 258:1812–1815.

Berridge, M. J. 1993. Inositol trisphosphate and calcium signalling. *Nature.* 361:315–325.

Chad, J. E., and R. Eckert. 1984. Calcium domains associated with individual channels can account for anomalous voltage relations of Ca-dependent responses. *Biophysical Journal.* 45:993–999.

Crabtree, G. R. 1989. Contingent genetic regulatory events in T lymphocyte activation. *Science.* 243:355–361.

Dolmetsch, R., and R. S. Lewis. 1994. Signaling between intracellular Ca^{2+} stores and depletion-activated Ca^{2+} channels generates $[Ca^{2+}]_i$ oscillations in T lymphocytes. *Journal of General Physiology.* 103:365–388.

Donnadieu, E., G. Bismuth, and A. Trautmann. 1992. Calcium fluxes in T lymphocytes. *Journal of Biological Chemistry.* 267:25864–25872.

Eckert, R., and J. E. Chad. 1984. Inactivation of Ca channels. *Progress in Biophysics and Molecular Biology.* 44:215–267.

Fasolato, C., B. Innocenti, and T. Pozzan. 1994. Receptor-activated Ca^{2+} influx: how many mechanisms for how many channels? *Trends in Pharmacological Sciences.* 15:77–83.

Fenwick, E. M., A. Marty, and E. Neher. 1982. Sodium and calcium channels in bovine chromaffin cells. *Journal of Physiology.* 331:599–635.

Gouy, H., D. Cefai, S. B. Christensen, P. Debré, and G. Bismuth. 1990. Ca^{2+} influx in human T lymphocytes is induced independently of inositol phosphate production by mobilization of intracellular Ca^{2+} stores. A study with the Ca^{2+} endoplasmic reticulum-ATPase inhibitor thapsigargin. *European Journal of Immunology.* 20:2269–2275.

Grinstein, S., and J. D. Smith. 1989. Ca^{2+} induces charybdotoxin-sensitive membrane potential changes in rat lymphocytes. *American Journal of Physiology.* 257:C197–C206.

Grissmer, S., R. S. Lewis, and M. D. Cahalan. 1992. Ca^{2+}-activated K^+ channels in human leukemic T cells. *Journal of General Physiology.* 99:63–84.

Hamill, O. P., A. Marty, E. Neher, B. Sakmann, and F. J. Sigworth. 1981. Improved patch-clamp techniques for high-resolution current recording from cells and cell-free membrane patches. *Pflügers Archiv.* 391:85–100.

Hoth, M., and R. Penner. 1992. Depletion of intracellular calcium stores activates a calcium current in mast cells. *Nature.* 355:353–356.

Hoth, M., and R. Penner. 1993. Calcium release-activated calcium current in mast cells. *Journal of Physiology.* 465:359–386.

Imredy, J. P., and D. T. Yue. 1992. Submicroscopic Ca^{2+} diffusion mediates inhibitory coupling between individual Ca^{2+} channels. *Neuron.* 9:197–207.

Kargacin, G. J. 1994. Calcium signaling in restricted diffusion spaces. *Biophysical Journal.* 67:262–272.

Lewis, R. S., and M. D. Cahalan. 1989. Mitogen-induced oscillations of cytosolic Ca^{2+} and transmembrane Ca^{2+} current in human leukemic T cells. *Cell Regulation.* 1:99–112.

Lewis, R. S., and M. D. Cahalan. 1995. Potassium and calcium channels in lymphocytes. *Annual Review of Immunology.* 13:623–653.

Lewis, R. S., P. E. Ross, and M. D. Cahalan. 1993. Chloride channels activated by osmotic stress in T lymphocytes. *Journal of General Physiology.* 101:801–826.

Lückhoff, A., and D. E. Clapham. 1994. Calcium channels activated by depletion of internal calcium stores in A431 cells. *Biophysical Journal.* 67:177–182.

Mason, M. J., C. Garcia-Rodriguez, and S. Grinstein. 1991. Coupling between intracellular Ca^{2+} stores and the Ca^{2+} permeability of the plasma membrane. Comparison of the effects of thapsigargin, 2,5-di-(tert-butyl)-1,4-hydroquinone, and cyclopiazonic acid in rat thymic lymphocytes. *Journal of Biological Chemistry.* 266:20856–20862.

Mason, M. J., B. Mayer, and L. J. Hymel. 1992. Inhibition of Ca^{2+} transport pathways in thymic lymphocytes by econazole, miconazole, and SKF 96365. *American Journal of Physiology.* 264:C654–C662.

McDonald, T. V., B. A. Premack, and P. Gardner. 1993. Flash photolysis of caged inositol 1,4,5-trisphosphate activates plasma membrane calcium current in human T cells. *Journal of Biological Chemistry.* 268:3889–3896.

Neely, A., R. Olcese, X. Wei, L. Birnbaumer, and E. Stefani. 1994. Calcium-dependent inactivation of a cloned cardiac calcium channel alpha-1 subunit expressed in *Xenopus* oocytes. *Biophysical Journal.* 66:1895–1903.

Neher, E. 1986. Concentration profiles of intracellular calcium in the presence of a diffusible chelator. *Experimental Brain Research Series.* 14:80–96.

Neher, E. 1988. The influence of intracellular calcium concentration on degranulation of dialysed mast cells from rat peritoneum. *Journal of Physiology.* 395:193–214.

Premack, B. A., T. V. McDonald, and P. Gardner. 1994. Activation of Ca^{2+} current in Jurkat T cells following the depletion of Ca^{2+} stores by microsomal Ca^{2+}-ATPase inhibitors. *Journal of Immunology.* 152:5226–5240.

Putney, J. W., Jr. 1990. Capacitative calcium entry revisited. *Cell Calcium.* 11:611–624.

Putney, J. W., Jr., and G. St. J. Bird. 1993. The inositol phosphate-calcium signaling system in nonexcitable cells. *Endocrine Reviews,* 14:610–631.

Roberts, W. M. 1993. Spatial calcium buffering in saccular hair cells. *Nature.* 363:74–76.

Robinson, R. A., and R. H. Stokes. 1955. Electrolyte Solutions. Butterworths, London 571 pp.

Sarkadi, B., A. Tordai, L. Homolya, O. Scharff, and G. Gárdos. 1991. Calcium influx and intracellular calcium release in anti-CD3 antibody-stimulated and thapsigargin-treated human T lymphoblasts. *Journal of Membrane Biology.* 123:9–21.

Sherman, A., J. Keizer, and J. Rinzel. 1990. Domain model for Ca^{2+}-inactivation of Ca^{2+} channels at low channel density. *Biophysical Journal.* 58:985–995.

Simon, S. M., and R. R. Llinás. 1985. Compartmentalization of the submembrane calcium activity during calcium influx and its significance in transmitter release. *Biophysical Journal.* 48:485–498.

Smith, S. J., and G. J. Augustine. 1988. Calcium ions, active zones and synaptic transmitter release. *Trends in Neurosciences.* 11:458–464.

Tsien, R. W., and R. Y. Tsien. 1990. Calcium channels, stores, and oscillations. *Annual Review of Cell Biology.* 6:715–760.

Tsien, R. Y. 1980. New calcium indicators and buffers with high selectivity against magnesium and protons: design, synthesis and properties of prototype structures. *Biochemistry.* 19:2396–2404.

Vaca, L., and D. L. Kunze. 1993. Depletion and refilling of intracellular Ca^{2+} stores induce oscillations of Ca^{2+} current. *American Journal of Physiology.* 264:H1319–H1322.

Zweifach, A., and R. S. Lewis. 1993. Mitogen-regulated Ca^{2+} current of T lymphocytes is activated by depletion of intracellular Ca^{2+} stores. *Proceedings of the National Academy of Sciences, USA.* 90:6295–6299.

Zweifach, A., and R. S. Lewis. 1994. Two mechanisms of Ca^{2+}-dependent inactivation of depletion-activated Ca^{2+} channels. *Biophysical Journal.* 66:A153. (Abstr.)